Kinetic evolution of blistering in hydrogen-implanted silicon

C. Coupeau, G. Parry, Jérôme Colin, M.-L. David, J. Labanowski, J. Grilhé

Kinetic evolution of blistering in hydrogen-implanted silicon

C. Coupeau, G. Parry, J. Colin, M.-L. David, J. Labanowski, and J. Grilhé

Citation: Applied Physics Letters **103**, 031908 (2013); doi: 10.1063/1.4813858
View online: http://dx.doi.org/10.1063/1.4813858
View Table of Contents: http://scitation.aip.org/content/aip/journal/apl/103/3?ver=pdfcov
Published by the AIP Publishing

Kinetic evolution of blistering in hydrogen-implanted silicon

C. Coupeau,[1,a)] G. Parry,[2] J. Colin,[1] M.-L. David,[1] J. Labanowski,[3] and J. Grilhé[1]
[1]*Institut P', UPR 3346 CNRS, Université de Poitiers-CNRS-ENSMA, France*
[2]*SIMAP, UMR 5266 CNRS, Université Joseph Fourier de Grenoble, France*
[3]*Institut IC2MP, UMR 7285 CNRS, Université de Poitiers, ENSIP, France*

(Received 23 May 2013; accepted 21 June 2013; published online 17 July 2013)

Silicon wafers have been implanted with hydrogen at high fluence. The kinetic evolution of the buckling structures has been observed *in situ* by atomic force microscopy during a thermal annealing at 200 °C. It is shown that the blistering of the silicon wafers occurs at the first stage of the annealing without any noticeable threshold. The deflection of the blisters continuously increases with time, and some blisters are observed to coalesce. The time evolution of the internal pressure inside the cavities is finally determined from the blister dimensions with the help of an elastic analytical model. © *2013 AIP Publishing LLC*. [http://dx.doi.org/10.1063/1.4813858]

Implantation of semiconductors by light ions such as hydrogen leads under specific conditions to the blistering of the free surfaces.[1,2] This phenomenon has found numerous technological applications such as the well-known layer splitting via ion cutting process used to produce silicon-on-insulator wafers.[3] It has been recently proposed as a way to produce p-Ge/n-Si diodes[4] or silicon surface textures for anti-reflexion purposes.[5] The possibility to transfer semiconductor thin films over a large variety of materials has been also found to be relevant with numerous applications.[6,7]

It is now well-established that the implantation process results in the first stage in the nucleation of nanodefects, the platelets, which may then evolve during thermal annealing.[8–11] These defects are supposed to be the precursors of the blistering phenomenon, with the appearance of micro-cavities in which the pressure subsequently increases by diffusion of the implanted species. Models based on the elastic theory have been developed by the past to estimate the internal pressure from the blister morphology and dimensions.[12–14] Moreover, recent analytical developments in the framework of the Foppl-von Karman theory have evidenced the combined effect of pressure and stress in the implanted layers on the resulting blister deflection.[15] Finite elements simulations allow also for taking into account plastic mechanisms that may occur in circular blisters.[16,17] No information is however still available concerning the kinetic evolution of the blisters during the thermal annealing. This is the aim of this letter to explore the evolution of the internal pressure as a function of the annealing time, which can give insight into the quantity of diffusing species in the implanted bulk materials.

N-type Czochralski-grown (001) Si wafers (200 μm thick) were first implanted normally to the surface at room temperature with hydrogen ions at $5 \times 10^{16}\,\mathrm{cm}^{-2}$ and 15 keV. The Si specimens were then annealed in air under the atmospheric pressure with a Peltier heater integrated to an atomic force microscopy (AFM) sample holder. The temperature was first increased as fast as possible (a few °C/min) up to 200 °C. This temperature was then maintained, and the surface was investigated *in situ* by atomic force microscopy in contact mode. The AFM probe has scanned continuously the surface over the 102 h of the experiment, and the scan rate was fixed so that one AFM image can be acquired every 3 min.

The kinetic evolution of the surface is shown in Fig. 1. For convenience, the AFM images are presented in error signal mode. This type of AFM images is not calibrated in the z axis but presents a great visual interest by fine detail enhancements. The scan size of each AFM image is $20 \times 20\,\mu\mathrm{m}^2$. The surface feature ("X" in Fig. 1(a)) can be used to position each image with respect to the others. As expected, the blistering phenomenon results in a distribution of circular structures homogeneously dispatched over the sample surface. The density of blisters first increases rapidly (see video linked at Fig. 1), so that the surface was saturated by blistered parts after only a few hours (Fig. 1(d)). The blisters continuously grew with the increasing time, and several coalescences of blisters then occur (for instance, see the transitions from α_1 (or β_1) to α_2 (or β_2) in Figs. 1(f)–1(h)). Finally, it is observed after approximately 45 h a "peeling" phenomenon of the blisters first appearing as a fine cut on the buckle (Fig. 1(j)). This feature develops then laterally so that a layer, only a few nanometer thick, was removed from all the blisters at the end of the annealing (102 h). This peeling phenomenon has been recently explained by means of chemical potential calculations, when surface diffusion is activated.[18] A competition between thinning down and cracking of the blisters was evidenced to be controlled by the internal pressure, and it is believed that the thin native oxide layer at the Si wafer plays a key role in the observed phenomenon.

The evolution of one characteristic blister (labelled A in Fig. 1(c)) during the first stage of the annealing time is shown in Fig. 2. Instead of a wide scattering of experimental data, it is observed that the blister radius, R, increases continuously up to approximately $t = 600$ min at which it remains roughly constant. This suggests that the delamination of the implanted layer rapidly extends laterally in the first stage and is afterwards strongly limited (or prohibited) by the surroundings blisters. A different behaviour is observed for the maximum deflection of the blister, δ. Contrary to the radius evolution, the blister deflection was evidenced to increase continuously. This behaviour was observed during the whole

a)christophe.coupeau@univ-poitiers.fr

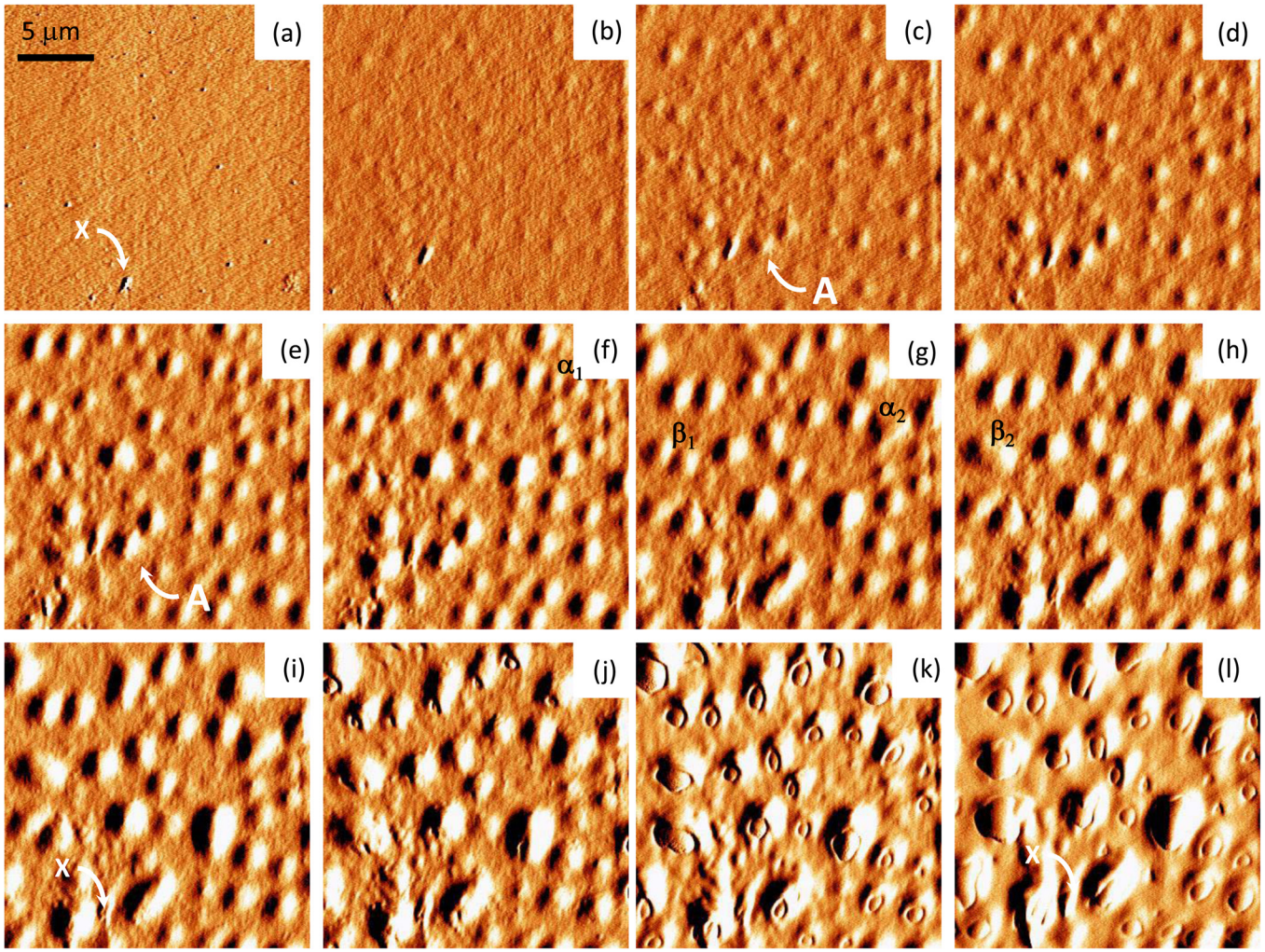

FIG. 1. Kinetic evolution of H-implanted Si surface during a thermal annealing at 200 °C. The scan size of the error signal mode AFM image is $20 \times 20\ \mu m^2$. The "X" surface feature can be used to position each AFM image from the others. (a) 2h36min, (b) 5h26min, (c) 6h59min, (d) 9h37min, (e) 13h38min, (f) 17h53min, (g) 26h20min, (h) 30h20min, (i) 34h20min, (j) 45h20min, (k) 62h28min, (l) 102 h (enhanced online) [URL: http://dx.doi.org/10.1063/1.4813858.1].

annealing. It can be consequently supposed that the hydrogen-diffusion is still active after more than 100 h of annealing at 200 °C. It is here underlined the nanometre scale of the deflection compared to the diameter of the blisters expressed in micrometers. This is characterized by a deflection over radius ratio, δ/R, lower than 1% during all the evolution. Finally, it is shown that the δ vs. t curve is characterized by several discontinuities that are regularly observed in the first stage of annealing (see τ_i events in Fig. 3(a)).

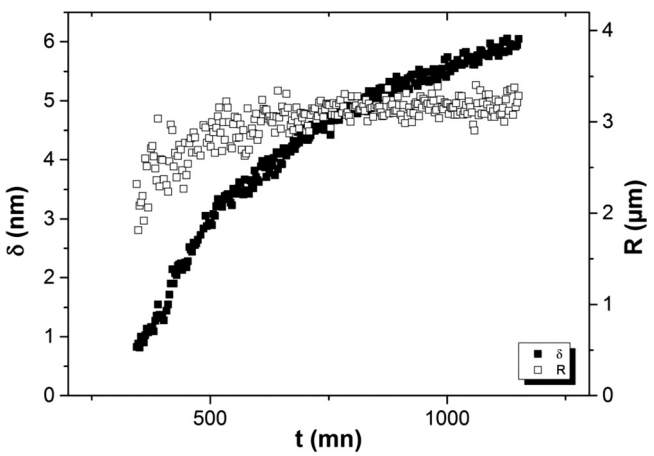

FIG. 2. Time evolution of the radius R and the maximum deflection δ of a characteristic blister during a thermal annealing at 200 °C.

The thickness of the delaminated/buckled layer was determined *post mortem* after a second thermal treatment at 450 °C during 30 min. Under these experimental conditions, the surface exhibits several circular holes that result from the exfoliation of the blisters.[15] The thickness h of the buckled layer was determined by AFM and found to be homogeneous and equal to 250 nm.

An analytical model has been developed to extract the time evolution of the internal pressure from the experimental results and the quantity of hydrogen diffusing into the microcavities beneath the blisters. A flat circular plate of thickness h and radius R is first considered, only submitted to an external pressure p_0 due to the atmosphere. The plate is considered as an isotropic and elastic solid in the following, with Young modulus E and Poisson ratio ν. A penny shape cavity of same radius lying underneath the plate is assumed to initially contain a negligible amount of hydrogen. As the gas diffuses into the cavity, the hydrogen quantity $N(t)$ increases leading to an increased value of the internal pressure $p(t)$. The deflection $\delta(t)$ of the blister increases as a result. The linear theory of thin plates is used to describe the elastic deformation of the

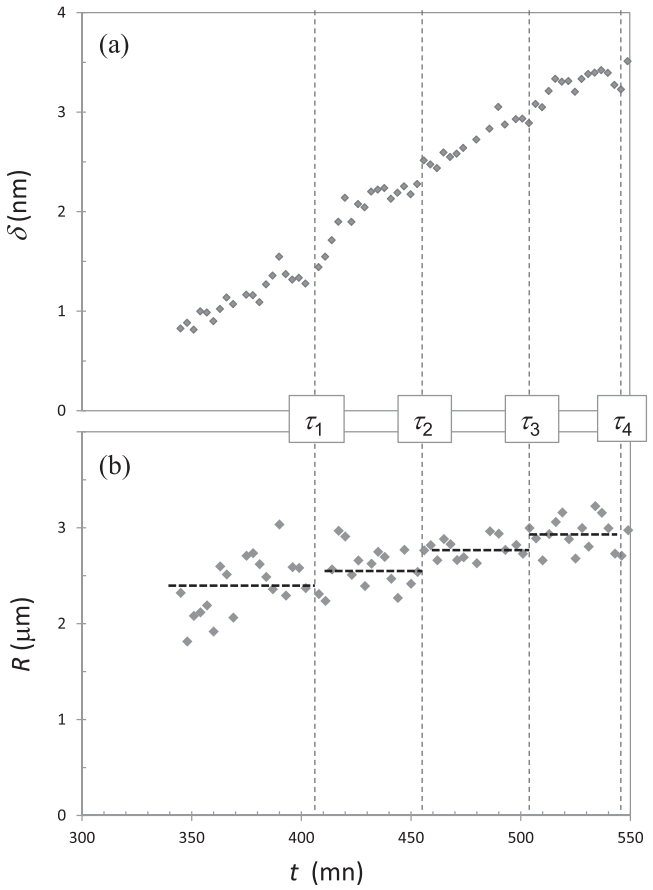

FIG. 3. First stage (enlargement of Fig. 2) of the kinetic evolution of a characteristic blister during a thermal annealing at 200 °C. (a) Maximum deflection δ and (b) radius.

blister. For convenience the effect of internal stresses in the implanted layers is not taken into account in the model. Under the above assumptions, the circular thin plate submitted to an internal pressure p and the external atmospheric pressure p_0 has the following out-of-plane displacement:[19,20]

$$w(r) = \frac{3}{16}\frac{(p-p_0)R^4}{\bar{E}h^3}\left(1-\frac{r^2}{R^2}\right)^2, \text{ with } \bar{E} = \frac{E}{1-\nu^2}. \quad (1)$$

The maximum deflection of the blister thus writes

$$\delta = w(0) = \frac{3}{16}\frac{(p-p_0)R^4}{\bar{E}h^3}. \quad (2)$$

Finally, using the expressions of the elastic strain energy W_e stored in the thin plate and the work of pressure W_p,[19,20] the energy release rate G of the blister can be written as

$$G = -\frac{1}{2\pi R}\left(\frac{\partial(W_e+W_p)}{\partial R}\right) = \frac{3}{32}\frac{(p-p_0)^2R^4}{\bar{E}h^3}. \quad (3)$$

When lateral growth of the blisters occurs (i.e., for $G=\Gamma$, with Γ the fracture energy), the effective volume underneath the blister increases. Depending on the diffusion rate compared to the crack velocity, the pressure may consequently decrease (or at least stay constant) leading to a maximum deflection that does no more increase with time. In this context, the discontinuities evidenced in Fig. 3(a) can be defined as the signatures at which the blister lateral growth occurred. Between the discontinuities, $G<\Gamma$; only the blister deflection evolution with constant radius is experimentally captured. In this case, the R vs. t evolution (Fig. 3(b)) should be characterized by a "step-like structure" for which the blister radius increases gradually by plateau with the increasing time. The average radius $\langle R \rangle$ of the characteristic blister for each τ_i domain has consequently been used in the following. $\langle R \rangle$ is found to be equal to 2.39 ± 0.31, 2.55 ± 0.17, 2.78 ± 0.13, 2.92 ± 0.18, and $3.11 \pm 0.13\,\mu$m in the successive domains (horizontal dotted lines in Fig. 3(b)).

The time evolution of the internal pressure is directly expressed as a function of the maximum deflection (Eq. (2)) by

$$p = p_0 + \frac{16}{3}\frac{\bar{E}h^3}{\langle R \rangle^4}\delta. \quad (4)$$

The internal pressure has been plotted in Fig. 4. It is shown that the pressure increases continuously in each domain, up to a maximum value at which significant drops are observed. Theses drops result from the occurrence of the lateral extension of the interfacial cracks (for $G=\Gamma$) leading to the sudden increase of the available volume below the blister. The critical pressure for interfacial crack extension is found roughly constant whatever the domains, ranging from 0.6 to 0.7 MPa. Finally, it was found that the blisters do not laterally extend anymore after τ_4 or only by coalescence phenomena mentioned previously. As the hydrogen diffusion is still active, the internal pressure in the microcavities below the blisters continuously increases with no more evidence of drops (Fig. 4). This strongly suggests that the exfoliation of the implanted surfaces already observed in a large variety of implanted materials[2,11,21] comes from a competition between the continuous increase of internal pressure below the blisters and a transversal fracture of the implanted layer all around the circular blisters.

In order to estimate the quantity of hydrogen, N, diffusing in the cavities, an ideal gas law is considered in the following. The volume V underneath the blister can be computed from Eq. (1) as[19,20]

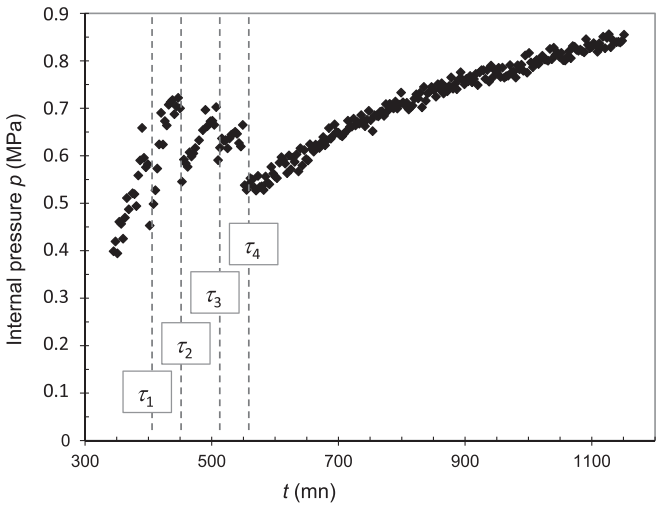

FIG. 4. Time evolution of the internal pressure p below a characteristic blister during a thermal annealing at 200 °C.

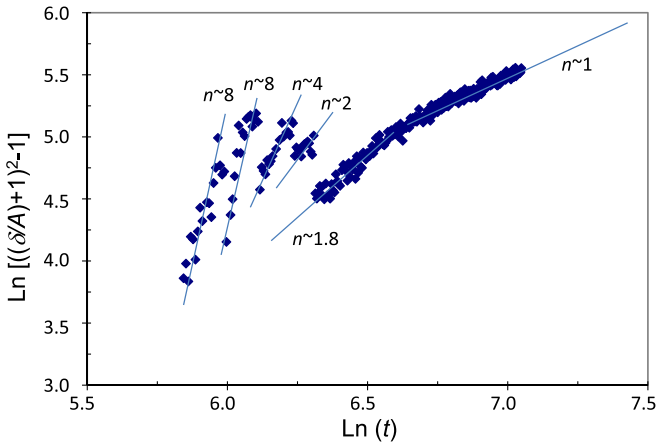

FIG. 5. $\ln\left[\left(\left(\frac{\delta}{A}\right)+1\right)^2-1\right]$ as a function of $\ln(t)$. The linear fit that corresponds to the diffusion coefficient n is given in each part of the graph.

$$V=\frac{1}{16}\frac{\pi(p-p_0)\langle R\rangle^6}{\bar{E}h^3}. \tag{5}$$

The internal pressure is thus given by

$$p=\frac{p_0}{2}\left\{1+\left(1+\frac{64kT\bar{E}h^3}{\pi\langle R\rangle^6 {p_0}^2}N\right)^{1/2}\right\}, \tag{6}$$

with T the temperature of the ideal gas and k the Boltzmann constant.

To explore the time dependence of diffusing hydrogen quantity, a diffusion law of the implanted species is supposed given by $N(t)=a.t^n$ in the following. Combining Eqs. (2) and (6), the maximum deflection writes for $G<\Gamma$

$$\delta(t)=\frac{3}{32}\frac{\langle R\rangle^4 \mathrm{p}_0}{\bar{E}h^3}\left(\left(1+\frac{64kT\bar{E}h^3 a}{\pi\langle R\rangle^6 {p_0}^2}t^n\right)^{1/2}-1\right). \tag{7}$$

Using $A=\frac{3}{32}\frac{\langle R\rangle^4 \mathrm{p}_0}{\bar{E}h^3}=cte$ and $B=\frac{64kT\bar{E}h^3 a}{\pi\langle R\rangle^6 {p_0}^2}=\mathrm{cte}$, $\ln\left[\left(\left(\frac{\delta}{A}\right)+1\right)^2-1\right]$ vs. $\ln(t)$ has been plotted in Fig. 5. By fitting the data with linear evolutions it is observed that the coefficient n that characterizes the diffusion law gradually decreases from the first stage of annealing ($n\sim 8$) to the final regime for which n reaches 1. It strongly suggests that different diffusion mechanisms could be activated in the hydrogen implanted material.

In conclusion, the evolution of blisters in hydrogen implanted silicon has been *in situ* observed during thermal annealing at 200 °C. In the framework of elasticity, the values of the internal pressure in microcavities embedded in the bulk materials have been extracted as a function of the annealing time. It is found that successive increases and drops of the pressure occur, supporting the idea of a competition between the hydrogen diffusion and the interfacial crack extension of blisters. The neighbourhood blisters then prohibit any further lateral extension leading to a continuous increase of the internal pressure. This explains the further exfoliation of free surfaces often reported in the literature, by transversal crack propagation at the circumference of the circular blisters. Finally, the time dependence of the quantity of hydrogen diffusing from the silicon bulk to the microcavities has been estimated from our modelling. It suggests that different diffusion mechanisms may occur in the early stage of annealing.

It is believed that experiments at higher in-plane resolution and temperature will give us insights into the various diffusion mechanisms taking place in implanted materials. Works are thus currently in progress to develop an original apparatus allowing to follow *in situ* by scanning tunnelling microscopy under ultra high vacuum environment the evolution of stressed surfaces in a large range of temperature, from 100 to 700 K.

The authors would like to thank Romain Boijoux (undergraduate student from the University of Poitiers) for performing the thorough statistical analysis of the morphological shapes of blisters. This work pertains to the French Government program "Investissements d'Avenir" (LABEX INTERACTIFS, reference ANR-11-LABX-0017-01).

[1]B. M. U. Sherzer, *Sputtering by Particle Bombardment II*, Topics in Applied Physics Vol. 52, edited by R. Behrisch (Springer, Berlin, 1983), p. 271.
[2]B. Terreault, Phys. Status Solidi A **204**, 2129 (2007).
[3]M. Bruel, Electron. Lett. **31**, 1201 (1995).
[4]F. Gity, K.-Y. Byun, K.-H. Lee, K. Cherkaoui, J. M. Hayes, A. P. Morrison, C. Colinge, and B. Corbett, Appl. Phys. Lett. **100**, 092102 (2012).
[5]N. Kadakia, S. Naczas, H. Bakhru, and M. Huang, Appl. Phys. Lett. **97**, 191912 (2010).
[6]O. Moutanabbir and U. Gösele, Annu. Rev. Mater. Res. **40**, 469 (2010).
[7]U. Dadwal and R. Singh, Appl. Phys. Lett. **102**, 081606 (2013).
[8]M. L. David, L. Pizzagalli, F. Pailloux, and J. F. Barbot, Phys. Rev. Lett. **102**, 155504 (2009).
[9]G. Moras, L. C. Ciacchi, C. Elsässer, P. Gumbsch, and A. De Vita, Phys. Rev. Lett. **105**, 075502 (2010).
[10]J. G. Swadener, M. I. Baskes, and M. Nastasi, Phys. Rev. B **72**, 201202 (2005).
[11]J. M. Zahler, A. F. i Morral, M. J. Griggs, H. A. Atwater, and Y. J. Chabal, Phys. Rev. B **75**, 035309 (2007).
[12]K. Mitani and U. Gösele, Appl. Phys. A **54**, 543 (1992).
[13]L. J. Huang, Q. Y. Tong, Y. L. Chao, T. H. Lee, T. Martini, and U. Gösele, Appl. Phys. Lett. **74**, 982 (1999).
[14]X.-Q. Feng and Y. Huang, Int. J. Solids Struct. **41**, 4299 (2004).
[15]C. Coupeau, E. Dion, M. L. David, J. Colin, and J. Grilhé, Eur. Phys. Lett. **92**, 16001 (2010).
[16]N. Enomoto, S. Muto, T. Tanabe, J. W. David, and A. Haasz, J. Nucl. Mater. **385**, 606 (2009).
[17]G. Parry, C. Coupeau, E. Dion, M. L. David, J. Colin, and J. Grilhé, J. Appl. Phys. **110**, 114903 (2011).
[18]C. Coupeau, J. Colin, M. L. David, and J. Grilhé, Scr. Mater. **65**, 672 (2011).
[19]J. W. Hutchinson and Z. Suo, Adv. Appl. Mech. **29**, 63 (1992).
[20]L. B. Freund and S. Suresh, *Thin Films Materials; Film Buckling, Bulging and Peeling* (University Press, Cambridge, 2003).
[21]J.-W. Hong, J.-H. Pyeon, J. W. Tedesco, and Y.-B. Park, Phys. Rev. B **75**, 214102 (2007).